study may shed new light on the roles of tau as well as *fukutin* in the developing human brain.

MATERIALS AND METHODS

Nine cases of FCMD were examined in this study, including 2 fetal cases (18 and 20 weeks gestational age) and 7 postfetal cases (14–34 years of age, with mean 22.9 ± 6.4 years of age, 6 males and one female). The profiles of the FCMD cases are summarized in Table 1. All postfetal cases had muscular dystrophy as well as brain malformation accompanied by a defect in the basal lamina, fulfilling the morphologic diagnostic criteria for FCMD (6, 9). Cases 1, 3, 4, 6, 7, and 8 were also used in our previous studies (6, 8). Two control fetal cases (23 and 24 weeks gestational age), 5 neurologically unremarkable age-matched postfetal cases (28–43 years of age, 3 females and 2 males), 5 AD cases (based on NIA-Ronald Reagan Institute Criteria) (18), and an 89-year-old man with incidental polymicrogyria served as controls. The 2 FCMD fetuses were aborted at their parents' request as a result of a prenatal diagnosis of FCMD based on the results of microsatellite polymorphism analysis of the fetal DNA (19, 20). The 2 control fetal cases were therapeutically aborted because of the maternal medical condition. Informed written consent for the use of the autopsy materials for research was obtained for all the cases examined.

Neuropathology

The brain, spinal cord, and pieces of skeletal muscle were sampled for examination. Half of the brain of case no. 1 and the frontal lobe of cases 2, 6, and 9 were kept frozen for biochemical and molecular studies. Pieces of the frontal lobe and the cerebellum from cases 2, 5, 6, and 9 were fixed in 2.5% glutaraldehyde for ultrastructural studies. Pieces of the frontal and occipital lobes and hippocampus from case no. 9 were fixed in 4% paraformaldehyde for 48 hours and embedded in paraffin. The rest of the brain and spinal cord were fixed in 10% buffered formalin and sliced in the coronal plane at approximately 8- to 10-mm thickness. After macroscopic observation, the appropriate areas were embedded in paraffin.

Six-μm-thick sections were stained with hematoxylin and eosin (H&E), Klüver-Barrera, and Bodian silver staining, periodic acid-methenamine (PAM), Watanabe, Bielschowsky, and Gallyas-Braak (21) methods.

Immunohistochemistry

After deparaffinization, 6-μm-thick sections were processed for single or double immunostaining using an automatic immunostainer (Ventana 20NX, Tucson, AZ) (22, 23). The following anti-tau antibodies were used for the study: AT8, phosphorylated Ser-202/Thr-205 (Innogenetics, Temse, Belgium); AP422, phosphorylated Ser-422 (a gift from Dr. Y. Ihara); and PHF1, Ser-396/404 (a gift from Dr. P. Davies). Also used were antiubiquitin (Sigma, St. Louis, MO), anti-Aβ (12B2, a.a. 11-28; IBL, Maebashi, Japan), antiphosphorylated α-synuclein (psyn#64, a gift from Dr. T. Iwatsubo), antiphosphorylated neurofilament (SMI 31; Sternberger Monoclonals Inc., Baltimore, MD), antimicrotubule-associated protein 2 (HM-2, Sigma), anticollagen type IV (CIV22; DAKO, Carpinteria, CA), antiglial fibrillary acidic protein (GFAP; Sigma), and antiHLADR (CD68; Sigma) antibodies. The specimens were prepared without the primary antibodies as negative controls.

Ultrastructural Study

Small pieces of the frontal lobe and cerebellar cortex from cases 1, 5, and 9 and the hippocampus from case 9 were fixed in 2% glutaraldehyde, postfixed in 1% osmium tetroxide, and embedded in epoxy resin. One-micrometer-thick semithin sections were stained with toluidine blue and an appropriate area was trimmed for ultrastructural observation.

Immunoelectron Microscopic Study

Ten percent buffered formalin-fixed, paraffin-embedded frontal lobe samples from the 2 fetal FCMD cases as well as the 2 controls were cut at 30-μm thickness, placed on Aclar film (Nisshin EM, Tokyo, Japan), and immunostained with

TABLE 1. Case Profiles of Fukuyama-Type Congenital Muscular Dystrophy

Case No.	Age	Gender	PMI (hours)	BW (g)	Gait	Epilepsy	Mutation in Fukutin Gene
1	18 gw	N/A	N/A	20†			Arg 47 Stop (exon3)/insertion
2	20 gw	M	4.2	40†			Insertion: homozygous
3	14 years	M	12	N/A	Impossible	−*	N/E
4	19 years	M	N/A	N/A	Ambulant until age 2 years	−	N/E
5	21 years	M	2	1,400	Impossible	+	Insertion: homozygous
6	21 years	M	2	1,350	Ambulant until age 9 years	−	Insertion: homozygous
7	24 years	M	5.5	1,160	Ambulant until age 7 years	+	N/E
8	27 years	F	N/A	N/A	Impossible	−*	N/E
9	34 years	M	5	1,350	Impossible	−	Insertion: homozygous

gw, gestational week; PMI (h), postmortem interval (hours); BW, brain weight; N/A, not available; Insertion, retrotransposal insertion; −*, electroencephalography showed abnormal discharge without epilepsy; N/E, not examined. †, The brain weight of normal controls (mean ± standard deviation) estimated by gestational weeks was 29.4 ± 8.4 g for 18 weeks and 45.5 ± 11.3 for 20 weeks ([33]).

antiphosphorylated tau protein (AT8 and AP422) using the avidin-biotin-peroxidase complex method (8). After the samples were fixed with 2% glutaraldehyde, postfixed in 1% osmium tetroxide, and embedded in epoxy resin, appropriate areas were trimmed and observed with an electron microscope (JEOL 2000EX, Tokyo, Japan). The specimens were prepared without the primary antibodies as negative controls.

Immunoblot Analysis of Phosphorylated tau

Sarkosyl-insoluble tau was extracted from fresh-frozen brains of patients with FCMD (cases 1 and 9), AD, and from a one-day-old rat. The tissues were homogenized with a polytron homogenizer in 10 volume (w/v) of buffer consisting of 10 mM Tris-HCl (pH 7.4), 0.8 M NaCl, 1 mM EGTA, and 10% sucrose and centrifuged for 15 minutes at 3,000 rpm (1,000 × g). The supernatants were retained and ultracentrifuged for 20 minutes at 800,000 rpm (390,000 × g). The pellets were resuspended in 10 volume (w/v) of homogenization buffer by sonication, brought to 1% Sarkosyl (w/v), and incubated for 1 hour at room temperature. After a 20-minute ultracentrifugation, the pellets were resuspended in 0.2 mL of 50 mM Tris-HCl (pH 7.4) per gram of starting material and used for immunoblotting. Aliquots were electrophoresed on 10% SDS-polyacrylamide gels, transferred to Immobilon membranes, and immunoblotted with anti-tau antibody, tau C (430-441), and HT7 (Innogenetics), and visualized by the avidin-biotin-peroxidase complex method (24, 25).

RESULTS

Macroscopic

Fetuses

The brain weight of the 2 fetal cases of FCMD was 20 g and 40 g, respectively. The surface of the brain showed extensive fine wrinkles over the cerebral cortex with frequent small verrucous regions (Fig. 1A, B) as has been previously reported (6).

Postfetal Cases

The brain weights of cases 5, 6, 7, and 9 were 1,400 g, 1,350 g, 1,160 g, and 1,350 g, respectively (Table 1). The brain weights of cases 3, 4, and 8 were not available. Bilateral cerebral and cerebellar polymicrogyria, accentuated in the frontal lobe and the cerebellar hemisphere, was seen to various degrees (Fig. 1C). Pachygyria involving the parietal and occipital lobes was also observed in cases 8 and 9 (not illustrated). In the serial coronal sections, fusion of the adjoining gyri was often present in the frontal lobe, where polymicrogyria was seen in all cases. In one of the control cases, incidental polymicrogyria with a similar structure was found in the parietal lobe.

Light Microscopy Study of Cortical Dysgenesis

Fetuses

The histologic features of both fetal cases of FCMD (Fig. 2) were essentially similar and therefore are described together. The cerebral cortex was diffusely covered by neurogliomesenchymal tissue (nGMT) (Fig. 2A, B) (6). The nGMT was thicker in case 2 than in case 1. The neuroglial elements located in the nGMT appeared to have migrated outward through multiple breaches of the glia limitans (Fig. 2B). The majority of the small blood vessels entered into the cortical plate from the nGMT through the breaches, although some of them appeared to penetrate into the cortical plate through intact segments of the glia limitans. In addition to heterotopic cortical plate neurons, the nGMT contained a few

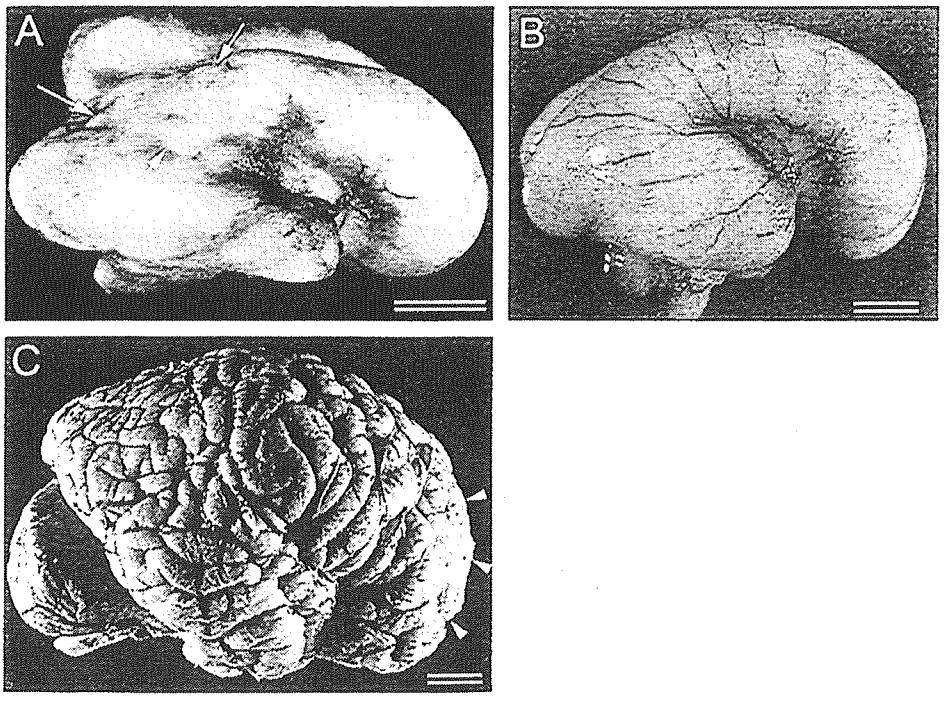

FIGURE 1. Macroscopic findings of the Fukuyama-type congenital muscular dystrophy brain. **(A)** A fetal case of Fukuyama-type congenital muscular dystrophy with extensive fine wrinkles over the cerebral cortex with frequent small verrucous regions (arrows) (case 2) Scale bar = 5 mm. **(B)** A normal control fetus (23-week gestational age). **(C)** A postfetal case (case 6) with typical polymicrogyria (arrowheads). Scale bar = 2 cm.

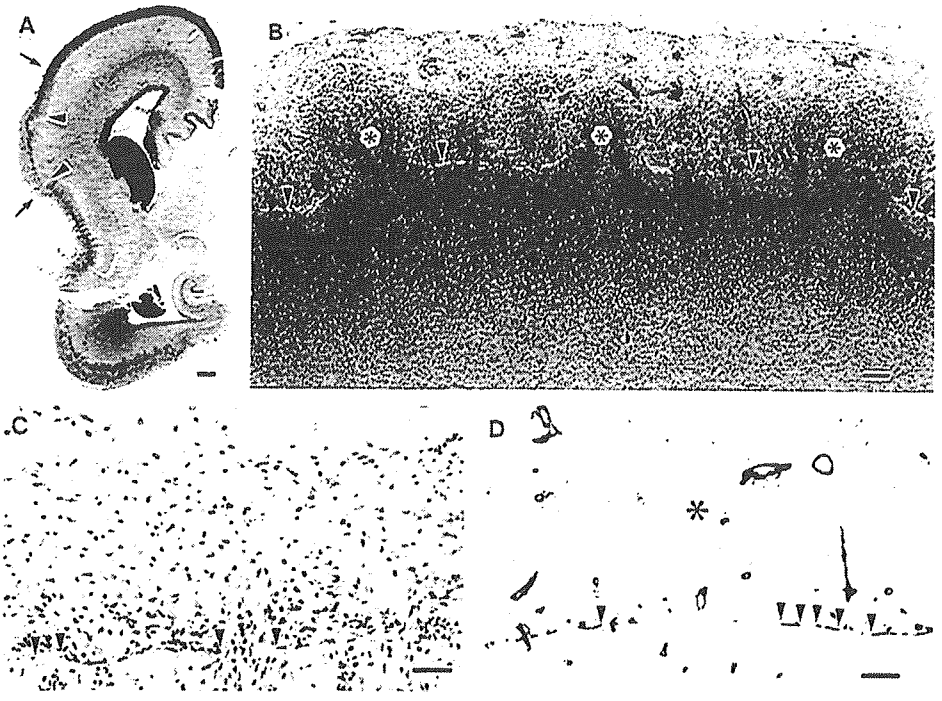

FIGURE 2. Microscopic findings of brain malformation in a fetal Fukuyama-type congenital muscular dystrophy case (case 2). **(A)** A coronal section of the left hemisphere at the hippocampus (hematoxylin & eosin). Gliomesenchymal tissue (arrows) with outer placement of the granular layer (arrowheads). Scale bar = 1 mm. **(B)** Higher magnification of the area indicated by arrowheads in the panel **(A)**. Asterisks indicate brain tissue protruding into the neurogliomesenchymal tissue (nGMT). Arrowheads indicate glia limitans (GL) and basal lamina (BL) complex. Scale bar = 100 μm. **(C)** Disruption of the GL-BL complex (arrowheads) visualized by GFAP immunostaining in the interface to the nGMT. Scale bar = 100 μm. **(D)** The disruption of the GL-BL complex detected immunohistochemically with anticollagen type IV antibody. Asterisk indicates nGMT and arrowheads show GL-BL complex. Scale bar = 100 μm.

deeply located Cajal-Retzius cells, subpial granular layer cells, and glial cells. In the parts of the cerebral cortex where the glia limitans was well preserved, the cortical architecture was normal. The breaches of the glia limitans were frequently detected in the frontal, temporal, and parietal lobes but were rare in the occipital cortex. In the cerebellum, the continuity of the outer granular cell layer was disrupted and clusters of granular cells were present in the subpial layer, where the cortex was covered by nGMT. In the cerebellar hemisphere, the structure partially resembled cerebellar polymicrogyria in the postfetal cases. The glia limitans in the cerebral cortex was immunoreactive to anticollagen type IV and GFAP antibodies, and had frequent breaches in the frontal, temporal, and parietal lobes (Fig. 2C, D).

Postfetal Cases

In the area with macroscopic polymicrogyria, nGMT (including neural and glial tissue) covered the brain surface. The adjoining gyri were fused by obliteration of the subarachnoid space with nGMT and the meningeal vessels were entrapped. Within this nGMT, haphazardly scattered ectopic neurons were detected, especially in the temporal lobe. In the immunohistochemical study, breaches of the glia limitans in the cerebral cortex were seen with anti-GFAP and collagen type IV antibodies. nGMT itself was also immunoreactive to anti-GFAP antibody.

Light Microscopy Study of Tauopathy

Fetuses

Gallyas-Braak silver staining was weakly positive in the neural tissue protruding from the breaches of the glia limitans, but no reaction was obtained with the Bodian or Bielschowsky method. In case 2, the argyrophilic structures appeared to be aggregated in the superficial layer of the nGMT. Immunohistochemically, AT8 and PHF1, which recognize the fetal phosphorylation site of tau, reacted with the parenchyma of both FCMD and control cases. However, AP422, which recognizes an abnormal phosphorylation site of tau that is present in AD but absent from fetuses (24), reacted only with the brains from FCMD cases (Fig. 3). The immunoreactivity was not observed in the negative controls processed without the primary antibodies (data not shown). The AP422-positive structures protruded from the breaches of the glia limitans and appeared to aggregate in the superficial layer of the nGMT in case 2. The AP422-immunoreactive structures in the nGMT were also stained with SMI 31 but not with anti-GFAP antibody, indicating that these structures were of neuronal, not glial, origin.

Postfetal Cases

NFTs and neuropil threads, visualized by silver staining, were present in the hippocampus, entorhinal and transentorhinal cortex, locus ceruleus, and basal nucleus of Meynert in all of the postfetal cases examined. The number and extent of NFTs were commensurate with age in cases 5, 6, 7, and 9. When the Braak staging for NFTs was applied, the younger cases (cases 5 and 6) were classified into the entorhinal stage, and the oldest case (case 9) was classified into the limbic stage (26). In addition, a small number of NFTs were scattered in the frontal and temporal lobes, cingulate gyrus, insular cortex, raphe nucleus, dentate nucleus, substantia nigra, and spinal anterior horn cells. Moreover, NFTs were also present in the ectopic neurons (Fig. 4A) within the abnormal nGMT. Swollen dendrites packed with NFTs were frequently seen (Fig. 4B).

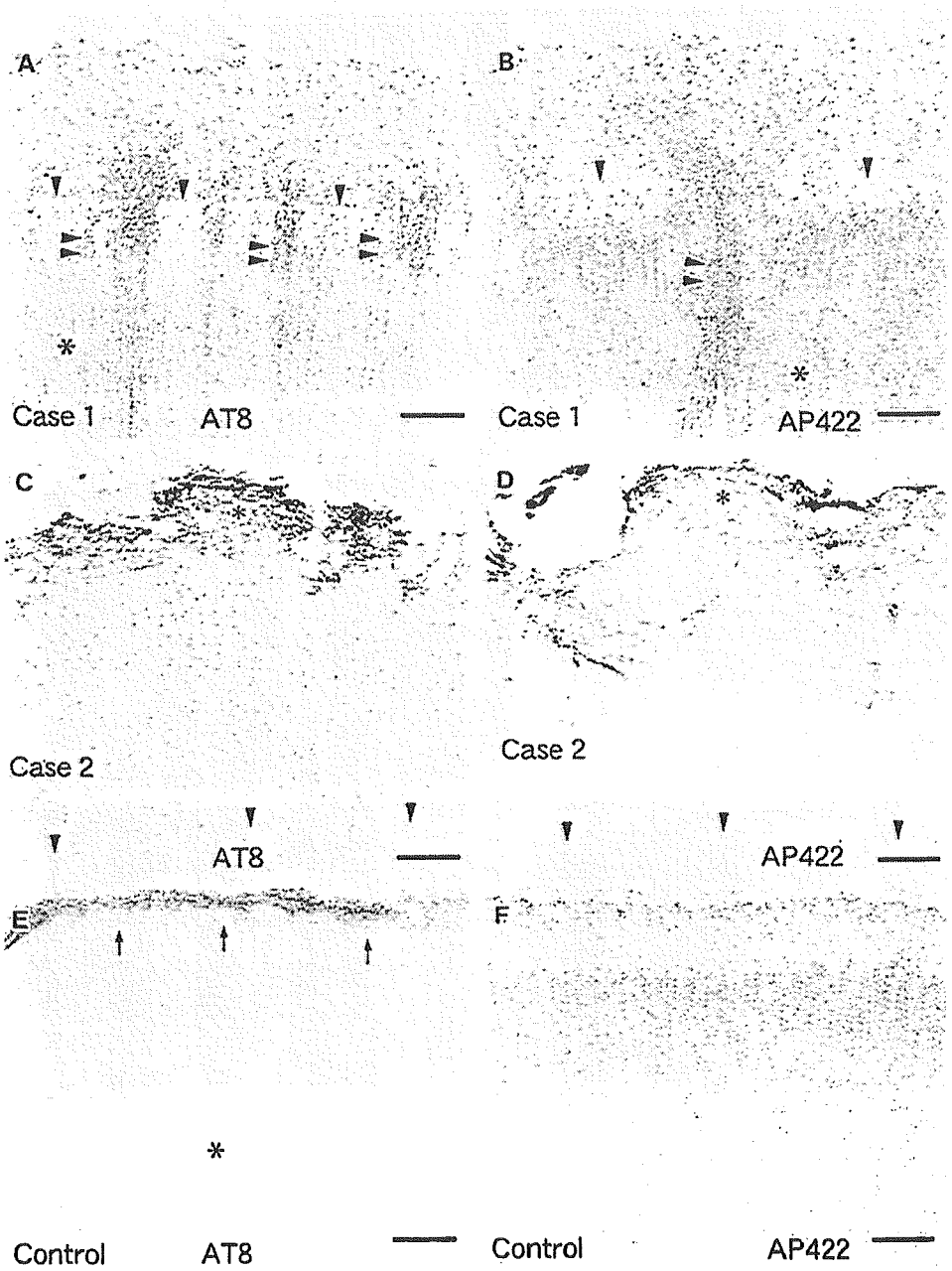

FIGURE 3. Tauopathy in the Fukuyama-type congenital muscular dystrophy fetal brains. **(A)** The AT8-immunoreactive protruding tissue (double arrowheads) from the parenchyma (asterisk) through breaches in the glia limitans (GL) and basal lamina (BL) complex (arrowheads, case 1). **(B)** The same pattern in immunostaining with AP422. Arrowheads indicate GL-BL complex and double arrowheads, protruding neural tissues from the brain parenchyma (asterisk). **(C)** AT8-immunoreactive ectopic tissue (asterisk). Arrowheads indicate GL-BL complex (case 2). **(D)** The same pattern in immunostaining with AP422. The asterisk indicates AP422-positive nGMT and arrowheads indicate GL-BL complex. **(E)** Superficial AT8 immunoreactivity in a control fetus. Arrows indicate the surface of the brain and asterisk, the deep cortical layer. **(F)** No immunoreactivity with AP422 in the control fetal brain (the same area in panel **[E]**). Scale bar = **(A–F)** 100 μm.

Immunohistochemical studies with antiphosphorylated tau antibodies detected more widespread abnormal structures than the silver staining methods in the malformed tissue as well as structures with apparently normal development in all the postfetal cases (Fig. 4C–G). The former included the area of the cortical fusion, nGMT, the ectopic neuronal tissue in the cerebral subpial layer, and the perivascular area (Table 2), including those in the younger cases (cases 3 and 4), but did not include the cerebellar polymicrogyria.

Neither anti-Aβ nor antiphosphorylated α-synuclein antibodies stained any structure. In the case of incidental polymicrogyria (89-year-old man), phosphorylated tau-positive

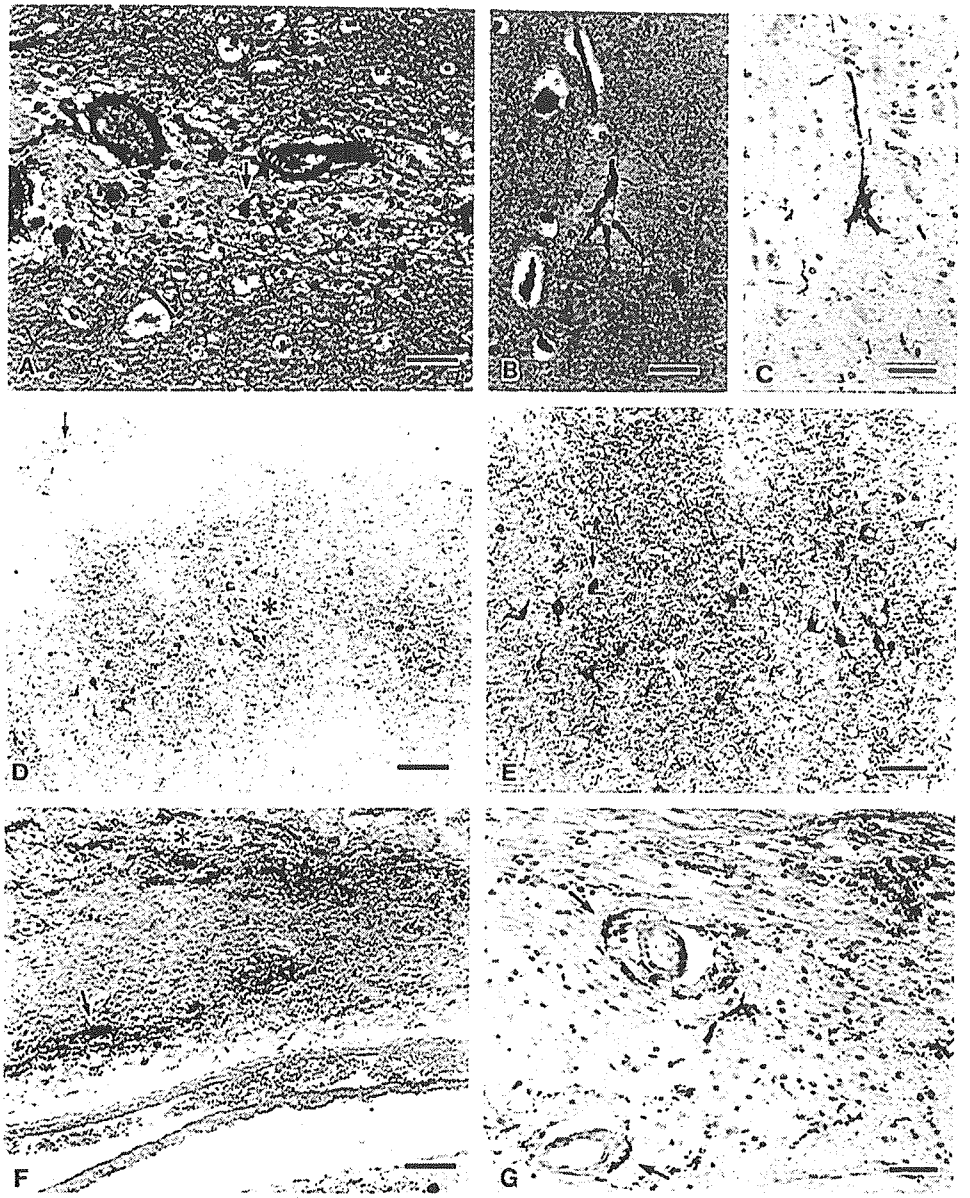

FIGURE 4. Tauopathy in postfetal cases of Fukuyama-type congenital muscular dystrophy. **(A)** Neurofibrillary tangles (NFT) (arrow) in the area of adhesion (case no. 8). Scale bar = 40 μm. **(B)** An NFT in an ectopic neuron in the hippocampus. Scale bar = 40 μm. **(C)** Serial section of panel **(B)**. AT8 immunostaining. Scale bar = 40 μm. **(D)** In addition to diffuse staining of the parahippocampal gyrus (asterisk), ectopic tissue including neuronal cytoplasm (arrow) shows AT8-immunopositive staining. Scale bar = 200 μm. **(E)** Neurofibrillary tangles (arrows) and neuropil threads visualized by AT8 immunostaining in the parahippocampal gyrus. Scale bar = 100 μm. **(F)** Ectopic tissue (asterisk) as well as perivascular area (arrow) showing positive AT8 immunostaining. Scale bar = 100 μm. **(G)** Ectopic tissue from the temporal lobe (AT8 immunostaining). The arrow indicates immunoreactive perivascular tissue. Scale bar = 100 μm.

structures were seen only in the entorhinal and transentorhinal areas, but not in the area of polymicrogyria.

Electron Microscopic Study

Fetuses

In the nerve processes protruding into the nGMT from the breaches of the glia limitans, bundles of microtubules were seen but no paired helical filaments (PHFs) were identified (Fig. 5A). An immunoelectron microscopic study demonstrated both AT8- and AP422-immunoreactive tubules in the same area (Fig. 5B). No immunostaining was detected either in the normal controls or the negative controls processed without the primary antibodies (data not shown).

Postfetal Cases

NFTs composed of PHFs were seen in the hippocampus from cases 7 and 8 (Fig. 6B). Anomalously shaped NFTs were only seen in FCMD cases. Hirano bodies (data not shown) and granulovacuolar changes were also seen in FCMD cases (Fig. 6A).

TABLE 2. Summary of Phosphorylated Tau-Related Structures in Relation to Cerebral Cortex

	Ptau-Immunoreactive Structures				Neurofibrillary Tangles			
Case No.	Limbic Regular	Limbic Ectopic	Neocortex Regular	Neocortex Ectopic	Limbic Regular	Limbic Ectopic	Neocortex Regular	Neocortex Ectopic
1	+	+	+	+	−	−	−	−
2	+	+	+	+	−	−	−	−
3	+	+	−	−	−	−	−	−
4	+	+	+/−	+/−	−	−	−	−
5	+	+	+	+	+	+	−	+
6	+	+	+	+	+	+	−	+
7	++	++	+	+	++	++	+	+
8	++	++	+	+	++	++	++	+
9	++	++	+	+	++	++	++	+

Ptau, phosphorylated tau.

Immunoblotting With Anti-tau Antibodies

A unique 50-kD band was present in a fetal FCMD case and was very weakly detected in a rat fetus used as a control (Fig. 7). In a postfetal case of FCMD (case 9), there were 3 major bands of tau: 60, 64, and 68 kD that were similar to pathologic tau in AD, plus some minor bands, as well as a 50-kD band similar to the 50-kD band observed in the fetal FCMD case. After dephosphorylation, the insoluble tau from

FIGURE 5. Ultrastructure of the antiphosphorylated tau-immunoreactive structure in a fetal case of Fukuyama-type congenital muscular dystrophy (case 1). **(A)** Higher magnification of the neural tissue protruding from glia limitans–basal lamina complex. Microtubules (asterisk) with focal constriction (arrows). Scale bar = 500 nm. **(B)** The tubules in the protruding tissue, decorated by AP422 (arrow) (avidin-biotin complex preembedding method). Scale bar = 500 nm. The decoration was abolished by skipping the application of APP422.

FIGURE 6. Ultrastructure of neurofibrillary tangles (NFT) in a postfetal case of Fukuyama-type congenital muscular dystrophy (case 6). **(A)** NFT-bearing neuron. "G" indicates the granulovacuolar degeneration. Scale bar = 500 nm. **(B)** Higher magnification of NFTs indicated in panel **(A)**, which consists of paired helical filaments (arrowheads) identical to those observed in Alzheimer disease. Scale bar = 200 nm.

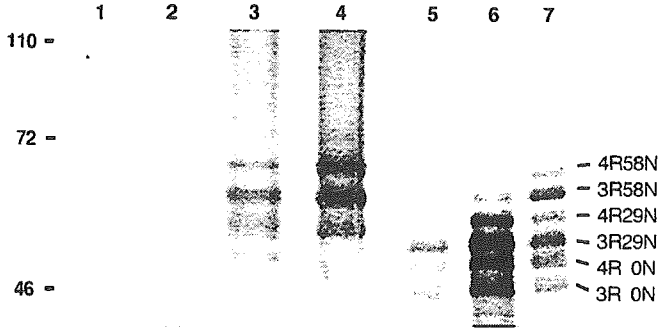

FIGURE 7. Biochemical analysis of tau in Fukuyama-type congenital muscular dystrophy (FCMD) brains. Immunoblots of sarkosyl-insoluble tau from one-day-old rat (lane 1), FCMD fetus (lane 2), FCMD postfetal case (lane 3), and Alzheimer disease (AD) (lane 4) brains with anti-tau antibody Tau C (430–441) and the sarkosyl-insoluble fraction after dephosphorylation stained with HT7. Note the presence of a 50-kD band in the fetal case of FCMD (lane 2), whereas there is only a very weak corresponding band in the fetal rat as a control (lane 1). In the postfetal case of FCMD (lane 3), 3 major tau bands of 60, 64, and 68 kD, which are similar to pathologic tau in AD (lane 4), plus some minor bands, as well as the 50-kDa band similar to that in the fetal FCMD case, were detected in the sarkosyl-insoluble fraction. After dephosphorylation, tau from the fetal (lane 5) and postfetal (lane 6) FCMD cases showed similar immunoblotting patterns and were richer in 3-repeat tau than was tau from AD (lane 7).

the fetus and the postfetal cases showed highly similar immunoblotting patterns and were more enriched in three-repeat tau than the insoluble tau from typical AD cases.

DISCUSSION

We report here for the first time a widespread tauopathy, or aberrant phosphorylation of tau, associated with brain malformation in fetal as well as postfetal cases of FCMD. The aberrant phosphorylation of tau in the malformed brain may be related to the abnormality of axonal development. It is not clear whether the 50-kDa band is of primary or secondary significance; however, it is common to both fetal and postfetal cases of FCMD. It is reasonable to assume that the 50-kD band observed in Western blots may correspond to the diffuse immunostaining in the neuropil of the malformed tissue with antiphosphorylated tau antibodies in both the fetal and the postfetal cases. Although only one fetal and one postfetal case were analyzed and no data were obtained for the brains of the control fetuses, the 50-kDa bands found in both in the fetal and postfetal FCMD are probably worthwhile reporting at this time in view of the difficulty of obtaining further tissues for analysis.

The location of aberrantly phosphorylated tau on structures similar to microtubules in the fetal case may indicate the loss of dynamic stability of microtubules in the abnormal environment. In FCMD cases, a tau band with an apparent molecular weight of 50 kDa was detected in the insoluble fraction. The lower molecular weight is likely to represent a lower level of tau phosphorylation because no degradation band was observed after dephosphorylation. These results suggest that the level of tau phosphorylation in the fetal stage, which is lower than the phosphorylation level in AD brains, may be sufficient to cause the accumulation of tau in FCMD brains. In FCMD, the aggregated (accumulated) tau may be converted to the filamentous form of the aggregates by further phosphorylation. It may also promote PHF formation by acting as a kind of seed.

The causative gene for FCMD has been shown to be expressed in developing neurons in the fetal brain by immunocytochemistry (27) and in situ hybridization (28), and is expressed at a lower level in the glia cells (29). More recently, congenital muscular dystrophies, which are said to be caused by defects in known or putative glycosyltransferases, have been shown to be commonly associated with hypoglycosylation of α-dystroglycan and a marked reduction of its receptor function (30). At present, fukutin is thought to play a cofactor role in glycosyl transfer at the Golgi membrane (Xiong et al, unpublished data). Because neuron-specific ligands for α-dystroglycan have been identified (31), fukutin may play a crucial role in neuronal migration by interacting with glycosyl residues in the matrix. Because several reports have indicated a direct link between abnormal protein glycosylation and aberrant phosphorylation of tau (32), fukutin could also play a role in the integrity of microtubules, a major cytoskeletal structure in neurite growth. Thus, the altered metabolism of tau in the malformed tissue of FCMD may represent a downstream event of the mutation of *fukutin* in the developing brain.

The phosphorylated insoluble tau from AD was reported to be similar to that from Niemann-Pick type C disease (16) but different from that from myotonic dystrophy (17). The phosphorylated tau from FCMD was apparently richer in three-repeat tau and less phosphorylated than that from AD. Although the formation of NFTs is a final common pathway of cytoskeletal alterations common to AD, the process of reaching that point may involve abnormal processing of tau that is specific to each original pathologic process. Thus, the study of tau in FCMD could provide new evidence about the pathogenesis of NFT formation.

ACKNOWLEDGMENTS

The authors thank Dr. Yasuo Ihara (Department of Neuropathology, University of Tokyo, Tokyo, Japan), Dr. Peter Davies (Department of Pathology, Albert Einstein College of Medicine, Bronx, New York), and Dr. Takeshi Iwatsubo (Department of Neuropathology and Neuroscience, Graduate School of Pharmaceutical Science, University of Tokyo, Tokyo, Japan) for the donation of antibody; Mr. Hiroyuki Kashima, Ms. Junko Saishoji, Mr. Naoo Aikyo, Ms. Mieko Harada, and Ms. Nobuko Naoi for the preparation of sections; and Dr. Kinuko Suzuki (Department of Pathology and Laboratory Medicine, University of North Carolina at Chapel Hill, North Carolina) for helpful discussions and comments. Part of this study was presented at the 80th Annual Meeting of the American Association of Neuropathologists, Inc. held in Cleveland, Ohio, June 2004.

REFERENCES

1. Fukuyama Y, Osawa M, Suzuki H. Congenital progressive muscular dystrophy of the Fukuyama type—Clinical, genetic and pathological considerations. Brain Dev 1981;3:1–29
2. Kamoshita S, Konishi Y, Segawa M, Fukuyama Y. Congenital muscular dystrophy as a disease of the central nervous system. Arch Neurol 1976; 33:513–16
3. Kobayashi K, Nakahori Y, Miyake M, et al. An ancient retrotransposal insertion causes Fukuyama-type congenital muscular dystrophy. Nature 1998;394:388–92
4. Barkovich AJ, Kuzniecky RI, Dobyns WB, Jackson GD, Becker LE, Evrard P. A classification scheme for malformations of cortical development. Neuropediatrics 1996;27:59–63
5. Takada K, Nakamura H, Tanaka J. Cortical dysplasia in congenital muscular dystrophy with central nervous system involvement (Fukuyama type). J Neuropathol Exp Neurol 1984;43:395–407
6. Nakano I, Funahashi M, Takada K, Toda T. Are breaches in the glia limitans the primary cause of the micropolygyria in Fukuyama-type congenital muscular dystrophy (FCMD)? Pathological study of the cerebral cortex of an FCMD fetus. Acta Neuropathol (Berl) 1996;9: 313–21
7. Yamamoto T, Shibata N, Kanazawa M, et al. Early ultrastructural changes in the central nervous system in Fukuyama congenital muscular dystrophy. Ultrastruct Pathol 1997;2:355–60
8. Saito Y, Murayama S, Kawai M, Nakano I. Breached cerebral glia limitans–basal lamina complex in Fukuyama-type congenital muscular dystrophy. Acta Neuropathol (Berl) 1999;98:330–36
9. Ishii H, Hayashi YK, Nonaka I, Arahata K. Electron microscopic examination of basal lamina in Fukuyama congenital muscular dystrophy. Neuromuscul Disord 1997;7:191–97
10. Takada K, Rin YS, Kasagi S, Sato K, Nakamura H, Tanaka J. Long survival in Fukuyama congenital muscular dystrophy: Occurrence of neurofibrillary tangles in the nucleus basalis of Meynert and locus ceruleus. Acta Neuropathol 1986;71:228–32
11. Oka A, Itoh M, Takashima S. The early induction of cyclooxygenase 2 associated with neurofibrillary degeneration in brains of patients with Fukuyama-type congenital muscular dystrophy. Neuropediatrics 1999;30: 34–37
12. Wisniewski K, Jervis GA, Moretz RC, Wisniewski HM. Alzheimer neurofibrillary tangles in diseases other than senile and presenile dementia. Ann Neurol 1979;5:288–94
13. Mandybur TI, Nagpaul AS, Pappas Z, Niklowitz WJ. Alzheimer neurofibrillary change in subacute sclerosing panencephalitis. Ann Neurol 1977;1:103–7
14. Suzuki K, Parker CC, Pentchev PG, et al. Neurofibrillary tangles in Niemann-Pick disease type C. Acta Neuropathol 1995;89:227–38
15. Autio-Harmainen H, Oldfors A, Sourander P, Renlund M, Dammert K, Simila S. Neuropathology of Salla disease. Acta Neuropathol (Berl) 1988; 75:481–90
16. Auer IA, Schmidt ML, Lee VM, et al. Paired helical filament tau (PHFtau) in Niemann-Pick type C disease is similar to PHFtau in Alzheimer's disease. Acta Neuropathol (Berl) 1995;90:547–51
17. Vermersch P, Sergeant N, Ruchoux MM, et al. Specific tau variants in the brains of patients with myotonic dystrophy. Neurology 1996;47:711–17
18. The National Institute on Aging, and Reagan Institute Working Group on Diagnostic Criteria for the Neuropathological Assessment of Alzheimer's Disease. Neurobiol Aging 1997;18(suppl):S1–2
19. Toda T, Miyake M, Kobayashi K, et al. Linkage-disequilibrium mapping narrows the Fukuyama-type congenital muscular dystrophy (FCMD) candidate region to 100 kb. Am J Hum Genet 1996;59:1313–20
20. Toda T, Ikegawa S, Okui K, et al. Refined mapping of a gene responsible for Fukuyama-type congenital muscular dystrophy: Evidence for strong linkage disequilibrium. Am J Hum Genet 1994;55:946–50
21. Gallyas F. Silver staining of Alzheimer's neurofibrillary changes by means of physical development. Acta Morphol Acad Sci Hung 1971;19:1–8
22. Grogan TM, Casey TT, Miller PC, Rangel CS, Nunnery DW, Nagle RB. Automation of immunohistochemistry. Adv Pathol Lab Med 1993;6:253–83
23. Grogan TM, Rangel C, Rimsza L, et al. Kinetic-mode, automated double-labeled immunohistochemistry and in situ hybridization in diagnostic pathology. Adv Pathol Lab Med 1995;8:79–100
24. Hasegawa M, Jakes R, Crowther RA, Lee VM, Ihara Y, Goedert M. Characterization of mAb AP422, a novel phosphorylation-dependent monoclonal antibody against tau protein. FEBS Lett 1996;384:25–30
25. Umeda Y, Taniguchi S, Arima K, et al. Alterations in human tau transcripts correlate with those of neurofilaments in sporadic tauopathies. Neurosci Lett 2004;359:151–54
26. Braak H, Braak E. Neuropathological staging of Alzheimer-related changes. Acta Neuropathol (Berl) 1991;82:239–59
27. Saito Y, Mizuguchi M, Oka A, Takashima S. Fukutin protein is expressed in neurons of the normal developing human brain but is reduced in Fukuyama-type congenital muscular dystrophy brain. Ann Neurol 2000; 47:756–64
28. Sasaki J, Ishikawa K, Kobayashi K, et al. Neuronal expression of the fukutin gene. Hum Mol Genet 2000;9:3083–90
29. Yamamoto T, Kato Y, Karita M, et al. Fukutin expression in glial cells and neurons: Implication in the brain lesions of Fukuyama congenital muscular dystrophy. Acta Neuropathol (Berl) 2002;104:217–24
30. Michele DE, Barresi R, Kanagawa M, et al. Post-translational disruption of dystroglycan-ligand interactions in congenital muscular dystrophies. Nature 2002;418:417–22
31. Sugita S, Saito F, Tang J, Satz J, Campbell K, Sudhof TC. A stoichiometric complex of neurexins and dystroglycan in brain. J Cell Biol 2001;154: 435–45
32. Liu F, Iqbal K, Grundke-Iqbal I, Hart GW, Gong CX. O-GlcNAcylation regulates phosphorylation of tau: A mechanism involved in Alzheimer's disease. Proc Natl Acad Sci U S A 2004;101:10804–9
33. Maroun LL, Graem N. Autopsy standards of body parameters and fresh organ weights in nonmacerated and macerated human fetuses. Pediatr Dev Pathol 2005;8:204–17

Neuropathology 2005; **25**, 165–170

Case Report

Argyrophilic grain disease presenting with frontotemporal dementia: A neuropsychological and pathological study of an autopsied case with presenile onset

Kenji Ishihara,[1,2] Shigeo Araki,[3] Nami Ihori,[4] Jun-ichi Shiota,[1] Mitsuru Kawamura,[2] Mari Yoshida,[5] Yoshio Hashizume[5] and Imaharu Nakano[6]

[1]Department of Neurology, Ushioda General Hospital, Kanagawa, [2]Department of Neurology, Showa University School of Medicine, Tokyo, [3]Department of Neurology, Kawasaki Cooperation Hospital, [4]Department of Rehabilitation, Kawasaki Cooperation Hospital, Kanagawa, [5]Department of Neuropathology, Institute for Medical Science of Aging, Aichi Medical University, Aichi and [6]Department of Neurology, Jichi Medical School, Tochigi, Japan

A right-handed Japanese man with no consanguinity exhibited personality changes, speech disorder and abnormal behaviors, such as stereotypical, running-away, environment-dependent, and going-my-way behaviors, since the age of 49 years. At age 52 years, neuropsychological examination revealed frontal lobe dysfunctions, mild memory impairment, and transcortical sensory aphasia. MRI showed symmetrical severe atrophy of the anterior part of the temporal and frontal lobes. The clinical diagnosis was FTD. He died at age 54 years after a clinical illness of approximately 5 years. Numerous argyrophilic grains were observed throughout the limbic system, temporal lobe, frontal lobe and brainstem. In addition, there were many tau-positive neurons and glial cells. These findings are all compatible with argyrophilic grain disease (AGD). Our case, however, is atypical AGD because of the young age of onset of the disease and sharply circumscribed cortical atrophy exhibiting severe neuronal loss and gliosis. Our case, together with some other similar cases of atypical AGD, gives rise to the possibility that this type of AGD would constitute a part of pathological background of FTD.

Key words: argyrophilic grain disease, frontotemporal dementia, tauopathy.

Correspondence: Kenji Ishihara MD, Department of Neurology, Ushioda General Hospital, Yako 1-6-20, Tsurumi-ku, Yokohama, Kanagawa 230-0001, Japan.
Email: k-ishihara@mvj.biglobe.ne.jp

Received 15 September 2004; revised 14 October 2004 and accepted 18 October 2004.

INTRODUCTION

FTD is a clinical syndrome, typically occurring in the presenium, arising from progressive degeneration of the frontal and temporal lobes. Pathologically, FTD is heterogeneous. Such diseases as Pick's disease with Pick bodies, corticobasal degeneration, PSP, neurofibrillary tangle dementia, dementia with motor neuron disease (motor neuron disease inclusion dementia, or amyotrophic lateral sclerosis with dementia), dementia lacking distinct histopathological features, and frontotemporal dementia with parkinsonism linked to chromosome 17[1] may present clinical features of FTD. Up to now, argyrophilic grain disease (AGD) has not been considered as a part of the pathological diagnosis in FTD.

Herein, we describe a case of AGD which was clinically diagnosed as having FTD, and we propose that a subgroup of AGD may constitute the pathological background of FTD.

Clinical summary

A 52-year-old right-handed Japanese man, with no history of significant past illness, was brought to our hospital by his wife because of his restlessness and abnormal speech. His family history was unremarkable. When he was 49 years old, he was involved in a traffic accident, and this was followed by several more accidents. At approximately the same time, his wife noticed that his character had begun to change and abnormal behavior had emerged. For example, he sent letters to his friends that were very boastful, he visited his old friends unexpectedly to annoy them, and he repeatedly went out and came home on his bicycle with no aim.

On examination, his general physical findings showed no abnormality. He was uncooperative during the neurological examination. He was disoriented for time and place, and he gave irrelevant answers to questions. He spoke in a low-pitched, monotonous voice. His muscle tone was normal and no involuntary movements were observed. No pathological grasping reflex was induced. His deep tendon reflexes were within the normal range. No cerebellar ataxia was observed. He exhibited abnormal behavior, such as stereotypical, running-away, environment-dependent, and going-my-way behaviors. He was ill tempered and had no insight into his illness. The results of neuropsychological tests, shown in Table 1, disclosed moderate dementia, frontal lobe dysfunction, memory impairment, and transcortical sensory aphasia (characterized by prominent naming disorder, literal paraphrasia, perseveration, fluent spontaneous speech, stereotyped contents, preserved repetition and reading, and preserved writing). His cognitive impairment was not severe, as he could point to objects correctly following verbal commands. Routine laboratory data were all within normal limits. MRI performed 6 months later revealed marked symmetrical atrophy of the anterior part of the temporal and frontal lobes (Fig. 1). During the clinical course of his disease, he showed abnormal behaviors, such as overeating and wandering, and was aggressive. Thereafter, he gradually became apathetic and lost weight, but he remained able to walk and was never bedridden. At the age of 54 years, he suddenly collapsed while eating his breakfast. He was transferred to the emergency unit in cardiopulmonary arrest state, but declared dead on arrival. The total clinical course of his disease was approximately 5 years. The clinical diagnosis was FTD.

Table 1 Results of neuropsychological test batteries performed in April 1999

WAIS-R	Verbal IQ	67
	Performance IQ	52
	Full scale IQ	56
WMS-R	Visual	51
	Attention/Concentration	83
	Other items	scale out
WCST	Accomplished category	1†
WAB	Aphasia quotient	78

†Performed category 1 means prominent perseveration and suggests frontal lobe dysfunction. WAB, western aphasia battery; WAIS-R, Wechsler adult intelligence scale-revised; WCST, Wisconsin card sorting test; WMS-R, Wechsler memory scale-revised.

Pathological findings

No malignancy was found in the visceral organs, but the patient was severely emaciated.

The fixed brain weighed 950 g. Macroscopic examination revealed circumscribed, knife-edge shape atrophy of the anterior temporal and frontal lobes bilaterally (Fig. 2). The lateral ventricles were dilated. The posterior half of the superior temporal gyrus was not atrophic. The substantia nigra and locus ceruleus were severely depigmented.

Sections of paraffin-embedded tissue were stained with HE, KB, Bodian, and Gallyas-Braak stains. In addition, immunohistochemistry was performed using anti-ubiquitin (Dako; Glostrup, Denmark; 1:100) and anti-tau (AT8; Innogenetics, Ghent, Belgium; 1:1000) antibodies.

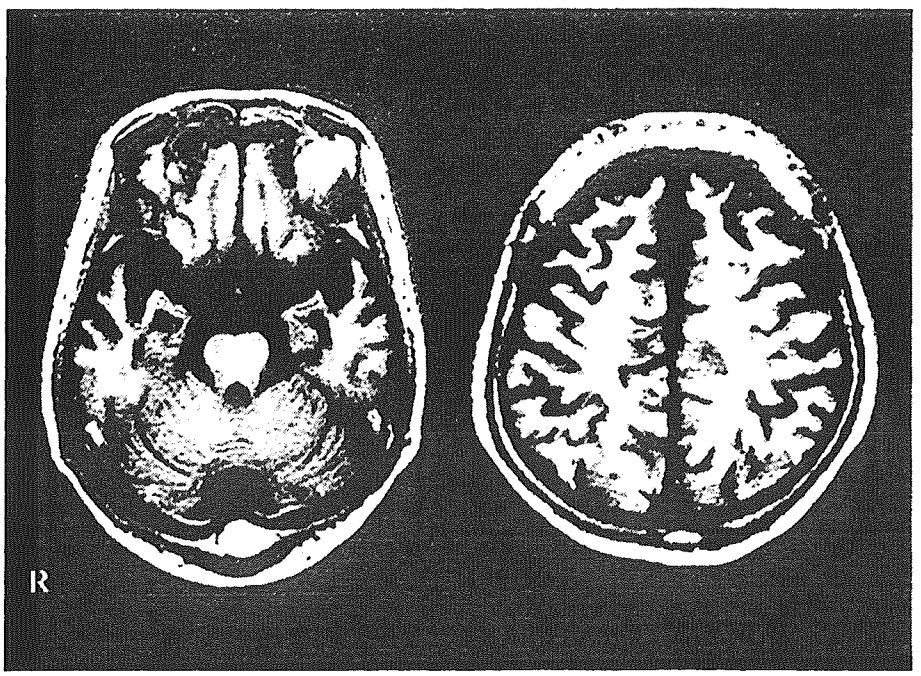

Fig. 1 MRI performed 6 months after the initial visit. Symmetrical atrophy of the both anterior temporal and frontal lobes can be seen.

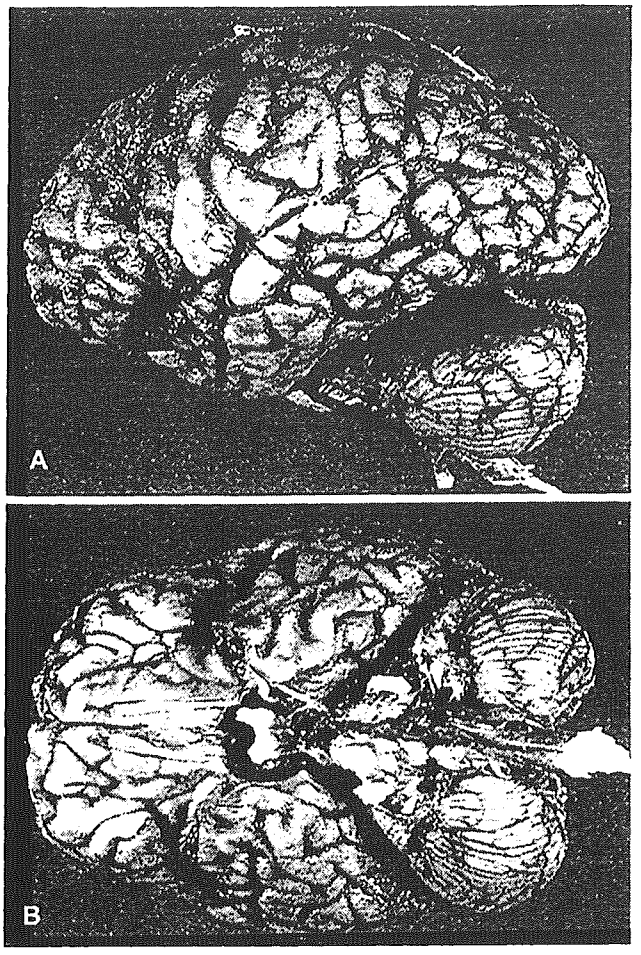

Fig. 2 Macroscopic appearance of the brain. Symmetrical, sharply circumscribed atrophy of the anterior temporal and frontal lobes can be seen. The posterior part of the temporal lobes was not atrophied. (A) Lateral view from the left side. (B) Basal surface of the cerebrum, brainstem, and cerebellum.

The outer layers of the temporal lobe cortex, from the parahippocampal gyrus to the superior temporal gyrus continuously, and the cortex of the frontal lobe convexity showed spongy state. Severe neuronal loss, gliosis and rarefaction of the neuropil were observed in the temporal lobe, being extremely severe in the rostral-medial part, in the transitional area between the CA1 subfield of the hippocampus and the subiculum, and in the amygdala. We found neither Pick bodies nor ubiquitin-positive intraneuronal inclusions. However, there were frequent ballooned neurons (BN), which were stained with anti-ubiquitin antibody, in the temporal and frontal lobes (Fig. 3A). There were few NFT, compatible with stage 1 of Braak and Braak.[2]

In the nucleus basalis of Meynert, pallidum, putamen, caudate nucleus, insular cortex, and cingulate gyrus, no remarkable changes were found with HE or KB stain.

The substantia nigra showed severe neuronal loss and gliosis with many BN and no Lewy bodies. The locus ceruleus showed mild neuronal loss and several BN. The cerebellum was unremarkable. There were no globose-type neurofibrillary tangles in the brainstem or cerebellum.

The most characteristic findings in this case were numerous argyrophilic grains (AG) and coiled bodies (CB), observed with Gallyas-Braak stain, in a widespread area, and numerous tau-positive neurons and glial cells. We found AG in the hippocampus, especially in the CA1 subfield (Fig. 3B), parahippocampal gyrus, adjacent temporal isocortex, amygdala, insular cortex, posterior cingulate gyrus, frontal lobe cortex (frontal convexity), and in the brainstem (midbrain and pons). There were numerous CB and fine argyrophilic threads in the white matter approximately subjacent to the cortical lesions (Fig. 3C), amygdala, thalamus, basal ganglia, subthalamic nucleus, posterior limb of the internal capsule, midbrain, pons, and cerebellum.

We also observed many tau-positive neurons and glial cells in the temporal lobe (Fig. 3D), midbrain, and pons. These tau-positive neurons were pretangles, as they appeared normal with HE stain and their cytoplasm was diffusely stained with AT8 antibody. Neither tufted astrocytes nor astrocytic plaques were found.

Pathologically, our case was diagnosed as AGD with severe temporal and frontal lobe atrophy, and widespread distribution of AG and CB.

DISCUSSION

FTD is characterized by profound alteration in personality and social conduct, and by cognitive defects in attention, abstraction, planning, judgement, organization and strategic functioning. Attenuation of conversational discourse leads ultimately to mutism, and is consistent with patients' amotivational state.[3,4] Atrophy of the frontal and temporal lobes are observed in MRI.[4] Abnormal behaviors, such as disinhibition, stereotypical, running-away, environment-dependent, and going-my-way behaviors, progressive speech disorder ultimately resulting in mutism, and personality changes observed in our case are typical features of FTD.[3,4] MRI findings also showed typical features of FTD. Thus, our case clinically masqueraded as FTD.

On the other hand, AGD is a progressive neurodegenerative disorder that is prevalent in the elderly.[5,6] It is distinct from other diseases, such as Alzheimer's disease, progressive supranuclear palsy, Pick's disease, and corticobasal degeneration.[7] Little has been reported on the clinical features of AGD.[5,6,8] However, some clinicopathological studies show that in AGD, inappropriate social conduct, such as marked restlessness, and personality changes, fea-

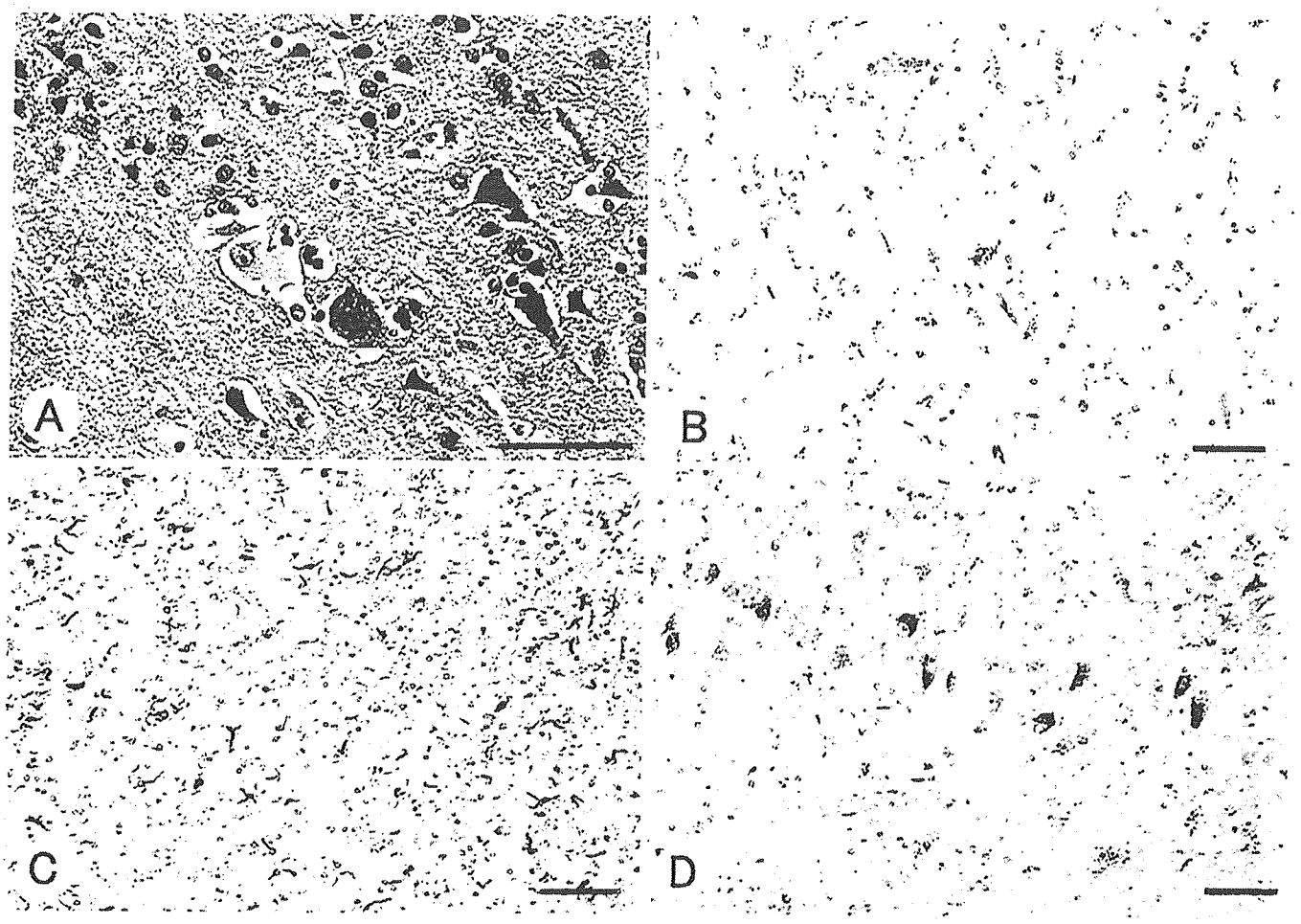

Fig. 3 Microscopic findings. (A) Ballooned neuron in the temporal lobe cortex. HE stain, Bar = 50 μm. (B) Numerous argyrophilic grains observed in the CA1 subfield of the hippocampus. Gallyas-Braak stain, Bar = 50 μm. (C) Numerous coiled bodies and argyrophilic threads observed in the temporal lobe subcortical white matter. Gallyas-Braak stain, Bar = 50 μm. (D) Many tau-positive neurons can be seen in the CA2 subfield of the hippocampal formation. AT8 immunostain, Bar = 50 μm.

turing an emotional disorder with aggression or ill temper, precede memory impairment and cognitive decline.[9,10,11]

The brains of patients with AGD may be macroscopically unchanged or only mildly atrophic, and do not differ from those of age-matched, mentally unimpaired controls.[5,9,12] Histologically, AGD features abundant AG, CB, BN, and pretangles.[5,10] AG, originally described by Braak and Braak as a novel neuropathological finding,[13,14] are abundant in the cortical neuropil, especially in the CA1 subfield of the hippocampus, the entorhinal and transentorhinal cortex, adjacent temporal isocortex, amygdala, and hypothalamic lateral tuberal nucleus.[12] The distribution of AG in the limbic system corresponds to the clinical features, that is, 'limbic dementia'.[10,11]

Our case revealed macroscopic pathological findings indistinguishable from that of FTD. Symmetrical cortical atrophy within the frontal and temporal lobes and relative sparing the superior temporal gyrus, especially posteriorly, are frequently observed in FTD.[4] The histopathology of our case, however, satisfies the criteria for the diagnosis of AGD. The combination of abundant AG in the limbic areas, CB in the white matter, BN in the cerebral cortex, and pretangles in the temporal lobe in our case are all compatible with the pathological diagnisis of AGD.[5,9,12] Although AG are also observed in other diseases, they are never as numerous as in AGD.[15] Moreover, our case lacks disease specific structures such as Pick's body, tufted astrocyte, and astrocytic plaque.

There are three other reports of cases with widespread distribution of AG and a clinical picture of FTD (Table 2).[8,16,17] Tanabe *et al.* reported a 60-year-old patient with a 16-year course of illness, who showed forgetfulness, stereotypical behavior, and antisocial behavior such as stealing.[16] Tsuchiya *et al.* reported an 89-year-old patient with a 15-year illness, who showed memory impairment, disorientation, character changes including violent, egocentric, stubborn behavior, and apathy.[8] CT showed atrophy of bilateral temporal lobes. Maurage *et al.* reported

Table 2 Previous case studies of argyrophilic grain disease presenting with FTD (Pick's disease)

Author (year)	Case (age at death/sex)	Clinical features	Clinical course (years)	Lesion distribution (AG and CB)
Tanabe *et al.* (1998)	60/male	Antisocial behaviors, memory impairment, oral tendency	16	F, T, BG, Ins, SN, Hip, Parahip
Tsuchiya *et al.* (2001)	89/female	Amnesia, wandering, character change (rude, stubborn, egocentric)	15	T, F, Ins, Cin, Amy, SN, LC, Hip, Parahip
Maurage *et al.* (2003)	76/female	Cognitive impairment, obsession, apathy, carbohydrate craving	14	T, F, P, O, Cin, Ins, BG, ST, Amy, Hip, Parahip
	79/female	Cognitive slowing, apathy, memory impairment, logorrhea, carbohydrate craving	7	T, F, P, O, Cin, Ins, BG, ST, Amy, SN, LC, Hip
Presented case	54/male	Character change (ill temper), abnormal behaviors (stereotypical, disinhibitory and environment-dependent)	5	T, F, Cin, Ins, BG, ST, Th, Amy, SN, LC Hip, Parahip

AG, argyrophilic grains; Amy, amygdala; BG, basal ganglia; CB, coiled bodies; Cin, cingulate gyrus; F, frontal lobe; Hip, hippocampus; Ins, insular cortex; LC, locus ceruleus; O, occipital lobe; P, parietal lobe; Parahip, parahippocampal gyrus; SN, substantia nigra; ST, subthalamic nucleus; T, temporal lobe; Th, thalamus.

two cases of atypical AGD.[17] A 76-year old patient with a 14-year illness presented with behavioral disturbances such as obsessions, carbohydroate craving, and apathy, in addition to cognitive impairment (case 1). CT scan showed atrophy of bilateral anterior temporal lobes. A 79-year-old patient with a 7-year illness showed carbohydrate craving, apathy, ansodiaphoria, loss of inhibition, and logorrhea in addition to cognitive slowing and memory impairment (case 2). MRI in the later stage showed diffuse atrophy of the brain cortex. Change in food preference, especially to sweet foods, is one of the characteristic clinical findings observed in FTD.[18] In these four cases, AG were observed not only in the limbic system but also in the frontal, temporal and parietal lobes, and the subcortical nuclei.

These four cases presented clinical pictures of FTD but were diagnosed as AGD pathologically. In spite of some clinicopathological differences, these cases and ours support the hypothesis that there is a subgroup of AGD indistinguishable from FTD clinically. Therefore, we think that this type of AGD would constitute a part of the pathological background of FTD.

REFERENCES

1. McKhann GM, Albert MS, Grossman M, Miller B, Dickson D, Trojanowski JQ. Clinical and pathological diagnosis of frontotemporal dementia. Report of the work group on frontotemporal dementia and Pick's disease. *Arch Neurol* 2001; **58**: 1803–1809.
2. Braak H, Braak E. Neuropathological stageing of Alzheimer-related changes. *Acta Neuropathol* 1991; **82**: 239–259.
3. Neary D, Snowden JS, Gustafson L *et al.* Frontotemporal lobar degeneration. A consensus on clinical diagnostic criteria. *Neurology* 1998; **51**: 1546–1554.
4. Snowden JS, Neary D, Mann DMA. *Fronto-Temporal Lobar Degeneration. Fronto-Temporal Dementia, Progressive Aphasia, Semantic Dementia.* New York: Churchill Livingstone, 1996.
5. Tolnay M, Monsch AU, Probst A. Argyrophilic grain disease. A frequent dementing disorder in aged patients. In: Tolnay M, Probst A (eds) *Neuropathology and Genetics of Dementia.* New York: Kluwer, 2001; 39–58.
6. Tolnay M, Probst A. Argyrophilic grain disease (AgD), a frequent and largely underestimated cause of dementia in old patients. *Rev Neurol (Paris)* 2002; **158**: 155–165.
7. Tolnay M, Schwietert M, Monsch AU, Staehelin HB, Langui D, Probst A. Argyrophilic grain disease: distribution of grains in patients with and without dementia. *Acta Neuropathol* 1997; **94**: 353–358.

8. Tsuchiya K, Mitani K, Arai T *et al.* Argyrophilic grain disease mimicking temporal Pick's disease: a clinical, radiological, and pathological study of an autopsy case with a clinical course of 15 years. *Acta Neuropathol* 2001; **102**: 195–199.
9. Braak H, Braak E. Argyrophilic grain disease: frequency of occurrence in different age categories and neuropathological diagnostic criteria. *J Neural Transm* 1998; **105**: 801–819.
10. Ikeda K, Akiyama H, Arai T *et al.* Argyrophilic grain dementia (Braak) – Clinicopathological evaluation of three cases (in Japanese with English abstract). *Shinkei Kenkyu no Shinpo* 1998; **42**: 855–866.
11. Ikeda K, Akiyama H, Arai T, Matsushita M, Tsuchiya K, Miyazaki H. Clinical aspects of argyrophilic grain disease. *Clin Neuropathol* 2000; **19**: 278–284.
12. Jellinger KA. Dementia with grains (argyrophilic grain disease). *Brain Pathol* 1998; **8**: 377–386.
13. Braak H, Braak E. Argyrophilic grains: characteristic pathology of cerebral cortex in cases of adult onset dementia without Alzheimer changes. *Neurosci Lett* 1987; **76**: 124–127.
14. Braak H, Braak E. Cortical and subcortical argyrophilic grains characterize a disease associated with adult onset dementia. *Neuropath Appl Neuro* 1989; **15**: 13–26.
15. Ikeda K, Akiyama H, Kondo H, Haga C. A study of dementia with argyrophilic grains. Possible cytoskeletal abnormality in dendrospinal portion of neurons and oligodendroglia. *Acta Neuropathol* 1995; **89**: 409–414.
16. Tanabe Y, Ishizu H, Terada S *et al.* Two cases of frontotemporal dementia and Klüver–Bucy syndrome with argyrophilic grains (Abstract). *Neuropathology* 1999; **19**: A23.
17. Maurage CA, Sergeant N, Schraen-Manschke S *et al.* Diffuse form of argyrophilic grain disease: a new variant of four-repeat tauopathy different from limbic argyrophilic grain disease. *Acta Neuropathologica* 2003; **106**: 575–583.
18. Ikeda M, Brown J, Holland AJ, Fukuhara R, Hodges JR. Changes in appetite, food preference, and eating habits in frontotemporal dementia and Alzheimer's disease. *J Neurol Neurosyurg Psychiatry* 2002; **73**: 371–376.

A phenotype without spasticity in sacsin-related ataxia

Abstract—The authors describe two Japanese siblings with autosomal recessive spastic ataxia of Charlevoix-Saguenay (ARSACS) without spasticity, usually a core feature of this disorder. They had a novel homozygous missense mutation (T987C) of the *SACS* gene, which resulted in a phenylalanine-to-serine substitution at amino acid residue 304.

NEUROLOGY 2005;64:2129–2131

H. Shimazaki, MD, PhD; Y. Takiyama, MD, PhD; K. Sakoe, PhD; Y. Ando, MD; and I. Nakano, MD, PhD

Autosomal recessive spastic ataxia of Charlevoix-Saguenay (ARSACS) (OMIM 270550) was originally found among inhabitants of the Charlevoix-Saguenay region of Quebec.[1] ARSACS is characterized by early-onset cerebellar ataxia, spasticity, peripheral neuropathy, foot deformity, and hypermyelinated retinal nerve fibers. Recently, the gene responsible for ARSACS (*SACS*) was identified in Quebec patients.[2] To date, 16 mutations including deletion, frame-shift, and missense ones have been reported in Quebec[2] and non-Quebec patients including ones in Japan,[3,4] Italy,[5,6] Tunisia,[7] and Turkey.[8]

Although there is some variation in symptom between Quebec and non-Quebec patients,[3-7,9] both groups usually have early-onset and lifelong spasticity. Here we present patients with ARSACS who have a novel *SACS* mutation but no spasticity.

Methods. We report two patients in a Japanese family with early-onset ataxia. The parents are second cousins and have two children, both affected. The family members, including the unaffected parents, underwent neurologic examination (HS).

We performed conventional nerve conduction studies on the sensory and motor nerves. Sensory nerves were examined by the antidromic stimulation technique.

Blood samples were obtained with informed consent from the two patients and their parents. Genomic DNA was extracted from peripheral blood leukocytes. Using 28 appropriate primer pairs (each primer sequence is available on request), the coding exon of the *SACS* gene was amplified by PCR from 200 ng of genomic DNA and then sequenced directly with an ABI PRISM 310 genetic analyzer; analysis was performed with Sequencing Analysis software, ver. 3.4.1 (ABI-Perkin Elmer).

When sequence analysis revealed a missense mutation, a T-to-C substitution at nt987, in the patients, we examined whether this transition existed in the chromosomes of 208 Japanese controls as follows. The PCR products with specific primers (741-F, 5'-AAGCTACTATTCGTCTGGC; 1187-R, 5'-GATCAGGACAAGCACCGA) were then digested with *Hpy188I* (New England BioLabs) at 37°C overnight, subjected to electrophoresis in 2% agarose gels, and then stained with ethidium bromide. Because the 987 T-to-C substitution results in the gaining of a *Hpy188I* restriction site, the PCR products with the missense mutation (T987C) gave two *Hpy188I*-digested bands (246 and 201 bp), whereas those without the mutation gave only one undigested band (447 bp).

This study was approved by the Medical Ethical Committee of Jichi Medical School.

Results. *Patient 1 (proband).* This 30-year-old man first walked at 18 months, his gait and running slow in the first decade. At age 20 years, he noticed unsteadiness of gait, which worsened gradually over 2 years. At age 28 years, the gait disturbance became worse again, and from age 30 years, he needed some assistance when walking. He had never felt his legs to be spastic, and his gait had not been described as spastic by his parents.

Neurologic examination at age 30 years revealed mild weakness of the lower extremities. Tendon reflexes were absent in all limbs, but the Babinski sign was present bilaterally. He exhibited no spasticity in the lower extremities. He showed limb and truncal ataxia and slurred and scanning speech. Saccadic eye movements and gaze-evoked nystagmus were noted. Vibratory sensation in the toes was reduced. He showed swan neck–like deformities of the fingers, hammer-toe deformity, and pes cavus. His gait was markedly ataxic but not spastic. Myelinated retinal nerve fibers were observed in the retina. A compound muscle action potential (CMAP) was not evoked in the common peroneal nerve. Motor nerve conduction velocity was mildly reduced in the ulnar and median nerves and moderately in the posterior tibial nerve. Each CMAP was markedly decreased. A sensory nerve action potential was not evoked in any of the extremities (table). Brain MRI revealed marked cerebellar atrophy with mega cisterna magna. His verbal IQ was 88 and his motor IQ was 61 (Wechsler Adult Intelligence Scale-Revised). A sural nerve biopsy revealed severe axonal degeneration and loss of large myelinated fibers, and a muscle biopsy disclosed marked neurogenic grouped atrophy in the short peroneal muscle.

Patient 2. This 32-year-old man is the elder brother of Patient 1. Although he first noticed gait unsteadiness at age 32 years, his gait had been slow since early childhood. He had never felt his legs to be spastic, and his gait had not been described as spastic by his parents. Neurologic examination at age 32 years revealed no spasticity in the lower extremities. Tendon reflexes were decreased with an absence of ankle jerks. The Babinski sign was present bilaterally. He showed mild limb and truncal ataxia and slurred speech but could walk without assistance. Saccadic eye movements and gaze-evoked nystagmus were noted. His foot deformities were similar to those of Patient 1. Motor nerve conduction velocity was mildly reduced in the

From the Department of Neurology (Drs. Shimazaki, Takiyama, Sakoe, Ando, and Nakano), Jichi Medical School, Tochigi, Japan.

This work was supported by a Research Grant for Nervous and Mental Disorders (14B, YT) and a grant from the Research Committee for Ataxic Diseases (YT) of the Ministry of Health, Labor and Welfare, Japan, and Grants-in-Aid for Scientific Research (C)(2) (15590903 [YT] and 15590905 [HS]) from the Ministry of Education, Science, Sports and Culture, Japan.

Received November 16, 2004. Accepted in final form March 3, 2005.

Address correspondence and reprint requests to Dr. Y. Takiyama, Department of Neurology, Jichi Medical School, Tochigi 329-0498, Japan; e-mail: ytakiya@jichi.ac.jp

Table *Peripheral neurophysiologic study*

	Patient 1		Patient 2		Normal	
	A	V*	A	V*	A	V
Motor						
Ulnar	2.9	32.3	4.0	40.0	9.1–21.9 (mV)	49–69 (m/s)
Median	3.6	41.9	3.4	45.0	4.6–19.0	47–60
Common peroneal	0	···	NE	NE	1.4–9.3	43–62
Posterior tibial	0.37	30.6	0.73	34.3	5.0–21.4	41–61
Sensory						
Ulnar (hand)	0	···	0	···	11.4–89.4 (μV)	46–60 (m/s)
Median (hand)	0	···	0	···	28.7–86.3	45–68
Sural	0	···	NE	NE	3.1–15.1	34–49

* Ellipses mean impossible to record.

A = amplitude; V = velocity; NE = not examined.

median and ulnar nerves and moderately in the posterior tibial nerve. Each CMAP was markedly decreased. A sensory nerve action potential was not evoked in any of the extremities (see table). The hypermyelination of the retinal nerve fibers was milder than that in Patient 1. Brain MRI revealed moderate cerebellar atrophy.

A homozygous missense mutation, a T-to-C transition at nt987, of the *SACS* gene was identified in the two patients (figure, C and D), which results in an original amino acid of phenylalanine-to-serine substitution at amino acid residue 304 (F304S). This substitution was found in the heterozygous state in the unaffected father and mother (see figure, A and B). Thus, the missense mutation of the *SACS* gene was found to cosegregate with the disease in the present family with autosomal recessive transmission. The T-to-C transition at nt987 was not found in 208 Japanese control chromosomes.

Although a T-to-C transition at nt7932 was identified in the homozygous state in the two patients and the heterozygous one in the parents, this transition was also found in the homozygous state in six of the 208 control chromosomes. Therefore, we consider that this transition is a benign single nucleotide polymorphism (SNP) as previously reported.[2]

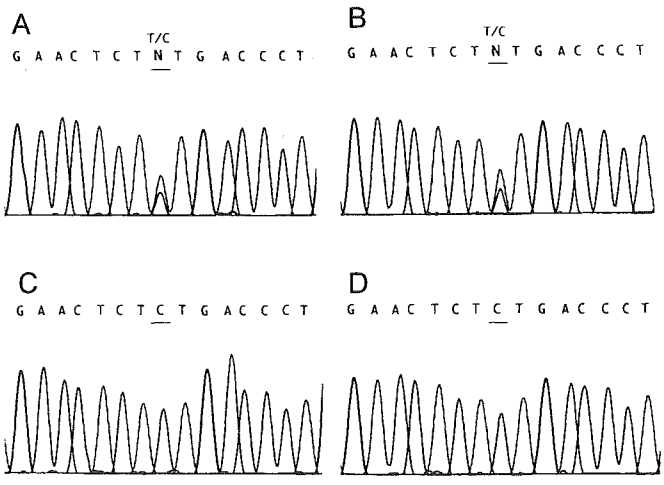

Figure. Identification of mutations of the SACS *gene. The sequences in the father (A), mother (B), Patient 2 (C), and Patient 1 (D) are shown. Underlining indicates the altered nucleotides: heterozygous T-to-C transition at nt987 in A and B and homozygous T-to-C transition at nt987 in C and D, resulting in a phenylalanine-to-serine substitution at amino acid residue 304 (F304S).*

Discussion. We consider the current new mutation (T987C) of the *SACS* gene responsible for our patients' condition for the following reasons. First, the mutation cosegregates with the disease in this family with autosomal recessive transmission. Second, T987C was not found in 208 Japanese control chromosomes. Third, phenylalanine 304 of sacsin is conserved in humans (AF193556) and mice (AF193557). Furthermore, F304S leads to a change in the secondary structure predicted by the PROF program.[10]

It is noteworthy that our patients lacked spasticity in the legs and showed areflexia or hyporeflexia. In Quebec and non-Quebec patients, spasticity becomes progressively worse during the disease and is prevalent in older patients, and tendon reflexes remain preserved throughout the disease, except for ankle jerks.[1,7] Since we could not observe our patients in childhood, it is possible that the reflexes have been lost in the course of the disease. Although the Babinski sign in our patients indicates pyramidal tract involvement, there is a possibility that the severe peripheral nerve degeneration, as shown by the biopsied sural nerve, masked any spasticity. Genetically, this leg spasticity–lacking phenotype might be associated with this new mutation of the *SACS* gene (F304S). In addition, the coding SNP (nt7932T→ C), which changed valine 2619 to alanine (V2619A) in our patients, might also be involved in the phenotypic variability. Our findings indicate that spasticity is not a constant feature of ARSACS, like mental retardation[3,5,6] and retinal myelination,[6,7] prompting us to examine the *SACS* gene even in cases of cerebellar ataxia without spasticity. Hereafter, as more *SACS* mutations are identified, the clinical spectrum of sacsinopathies will most likely expand. A further genotype-phenotype correlation

study will shed light on the molecular mechanism underlying ARSACS.

Acknowledgment

The authors thank the family for participating in this study. They also thank Dr. Mikiko Takezawa, Department of Ophthalmology, Jichi Medical School, and Dr. Shinsuke Yokoyama, Department of Ophthalmology, Sano Kosei General Hospital, for photographs of the patients' retinas.

References

1. Bouchard JP, Barbeau A, Bouchard R, Bouchard RW. Autosomal recessive spastic ataxia of Charlevoix-Saguenay. Can J Neurol Sci 1978;5:61–68.
2. Engert JC, Bérubé P, Mercier J, et al. ARSACS, a spastic ataxia common in northeastern Québec, is caused by mutations in a new gene encoding an 11.5-kb ORF. Nat Genet 2000;24:120–125.
3. Ogawa T, Takiyama Y, Sakoe K, et al. Identification of a *SACS* gene missense mutation in ARSACS. Neurology 2004;62:107–109.
4. Hara K, Onodera O, Endo M, et al. Sacsin-related autosomal recessive ataxia without prominent retinal myelinated fibers in Japan. Mov Disord 2005;20:380–382.
5. Criscuolo C, Banfi S, Orio M, et al. A novel mutation in *SACS* gene in a family from southern Italy. Neurology 2004;62:100–102.
6. Grieco GS, Malandrini A, Comanducci G, et al. Novel *SACS* mutations in autosomal recessive spastic ataxia of Charlevoix-Saguenay type. Neurology 2004;62:103–106.
7. El Euch-Fayache G, Lalani I, Amouri R, et al. Phenotypic features and genetic findings in sacsin-related autosomal recessive ataxia in Tunisia. Arch Neurol 2003;60:982–988.
8. Richter AM, Ozgul RK, Poisson VC, et al. Private SACS mutations in autosomal recessive spastic ataxia of Charlevoix-Saguenay (ARSACS) families from Turkey. Neurogenetics 2004;5:165–170.
9. Richter A, Rioux JD, Bouchard JP, et al. Location score and haplotype analyses of the locus for autosomal recessive spastic ataxia of Charlevoix-Saguenay, in chromosome region 13q11. Am J Hum Genet 1999;64:768–775.
10. Rost B, Sander C. Prediction of protein secondary structure at better than 70% accuracy. J Mol Biol 1993;232:584–599.

Expert Opinion

Gene Therapy

Gene therapy for Parkinson's disease using recombinant adeno-associated viral vectors

Shin-ichi Muramatsu†, Hideo Tsukada, Imaharu Nakano & Keiya Ozawa
†Jichi Medical School, Division of Neurology, Department of Medicine, 3311-1 Yakushiji, Minami-kawachi, Tochigi, 3290498 Japan

Existing strategies for gene therapy in the treatment of Parkinson's disease include the delivery of genes encoding dopamine (DA)-synthesising enzymes, leading to localised production of DA in the striatum; genes encoding factors that protect nigral neurons against ongoing degeneration, such as glial cell line-derived neurotrophic factor; and genes encoding proteins that produce the inhibitory transmitter γ-aminobutylic acid (GABA) in the subthalamic nucleus (STN), thus suppressing the hyperactive STN. Recombinant adeno-associated viral (rAAV) vectors, which are derived from non-pathogenic viruses, have been shown to be suitable for clinical trials. These rAAVs have been found to transduce substantial numbers of neurons efficiently and to express transgenes in mammalian brains for long periods of time, with minimum inflammatory and immunological responses. *In vivo* imaging using positron emission tomography is useful for monitoring transgene expression and for assessing the functional effects of gene delivery. Vector systems that regulate transgene expression are necessary to increase safety in clinical applications, and the development of such systems is in progress.

Keywords: AAV, adeno-associated virus, dopamine, gene therapy, glial cell line-derived neurotrophic factor, Parkinson's disease, positron emission tomography

Expert Opin. Biol. Ther. (2005) 5(5):663-671

1. Introduction

Parkinson's disease (PD) is a common neurodegenerative disorder among the elderly, with an estimated prevalence of 1% in individuals > 60 years old. During the progression of PD there is a loss of neurons in the substantia nigra pars compacta (SNc), which projects to the striatum (caudate and putamen), leading to a substantial decrease in the dopamine (DA) content of the striatum. Although our understanding of the molecular basis of PD has advanced following the identification of mutations in the *α-synuclein*, *parkin*, *DJ-1*, *PINK1* and *LRRK2* genes associated with familial PD [1-3], the cause of PD largely remains unknown and to date there is no curative therapy.

The primary symptoms of PD are motor disturbances, including resting tremor, muscular rigidity and bradykinesia. These symptoms become apparent after 40 – 50% of the neurons in the SNc have been lost and striatal DA has been reduced to ~ 20% of normal levels [4]. The introduction of the DA precursor L-3,4-dihydroxyphenylalanine (L-dopa) in the late 1960s represented a major therapeutic advance in the management of PD, demonstrating that the replacement of DA is important in alleviating the motor symptoms of this disease. Although virtually all PD patients benefit clinically from L-dopa therapy, L-dopa becomes less effective as the disease progresses. Frequent systemic administration of high-dose L-dopa causes oscillations in motor performance [5,6] and deleterious

complications, including hallucinations due to dopaminergic stimulation of the mesolimbic system [7]. Thus, novel therapeutic interventions that complement or substitute for oral L-dopa administration are required.

Unlike other neurological disorders that affect broad regions of the brain, PD is primarily confined to the well-defined nigrostriatal dopaminergic system. Stereotactic techniques based on microelectrode recording of neural activities and magnetic resonance imaging-assisted navigation have become established in clinical practice and can be used in gene therapy to deliver vectors into the striatum.

2. Recombinant adeno-associated viral vectors

Among the various gene delivery vehicles tested preclinically for PD, the recombinant adeno-associated viral (rAAV) vector has been found most suitable for clinical applications, due to both its efficacy and safety. This vector is the only one based on the use of a non-pathogenic and replication-defective virus. Efficient and long-term gene expression has been achieved in mammalian brains without substantial toxicity or immune response [8-11]. Wild-type adeno-associated viruses (AAVs) are small, non-enveloped, single-stranded DNA viruses of the *Parvoviridae* family assigned to the genus *Dependovirus*. Productive infection with AAV has been found to require coinfection with a helper virus, such as adenovirus or herpes virus [12]. Until the mid-1990s, only AAV serotype 2 (AAV-2) had been sequenced, making it a major platform for gene therapy vector development [13-20]. So far > 100 different AAV sequences have been isolated from human and non-human primates [21], and their recombinants have been investigated extensively for tissue tropism and transduction efficiency. This has led to an increase in transduction efficiency, as well as being associated with changes in tissue or cell type tropism or vector distribution patterns in a given tissue [22-26].

Although chromosomal rearrangements in association with rAAV integration have been observed in a transformed cell line [27] and in regenerating hepatocytes [28], rAAV is more commonly present *in vivo* as duplex, circular and head-to-tail concatemers, most of which are episomal in non-dividing cells in the absence of selection [29]. Preferential integration into active regions of the chromosome and into actively transcribed genes is not unique to rAAV vectors [30], inasmuch as it has been noted even in adenoviruses, which are generally considered to be non-integrating. In addition, the promoter activity of the terminal repeat sequence of AAV is much weaker than that of retrovirus, probably limiting transcription to the inward direction of the viral genome. Thus, the risks of insertional mutagenesis and activation of oncogenes are quite low. Other safety aspects of rAAV vectors have been reviewed elsewhere [31,32].

Pre-existing antibodies to naturally infecting AAV-2 are found in 80% of the human population, and neutralising antibodies can be induced after rAAV vector administration. These antibodies may compromise transgene expression [33,34], and the presence of elevated neutralising antibody titres should be considered as exclusion criteria for clinical trials, although further studies are necessary to more specifically define the antibody titre that would constitute exclusion. Different rAAV vector serotypes will permit successful retransduction in response to significant levels of neutralising antibodies to one or more rAAV vectors.

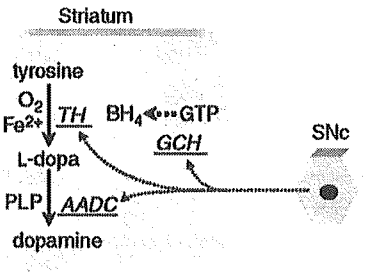

Figure 1. Biosynthetic pathway of DA. Three enzymes are necessary for efficient DA production. TH converts dietary tyrosine into L-dopa, which in turn is converted into DA by AADC. GCH is the rate-limiting enzyme for the biosynthesis of BH_4, the essential TH cofactor. All three of these enzymes are synthesised in the substantia nigra and transported to the striatum. Drastic reduction in the activities of these enzymes results in the depletion of DA in the striatum, leading to the manifestation of motor symptoms.
AADC: Aromatic-L-amino acid decarboxylase; BH_4: Tetrahydrobiopterin; DA: Dopamine; GCH: Guanosine triphosphate cyclohydrolase I; GTP: Guanosine triphosphate; L-dopa: L-3,4-dihydroxyphenylalanine; PLP: Pyridoxal 5'-phosphate; SNc: Substantia nigra pars compacta; TH: Tyrosine hydroxylase.

3. Local production of dopamine in the striatum

3.1 Biosynthesis of dopamine

One potential strategy of gene therapy for PD is to restore local production of DA by delivering genes of DA-synthesising enzymes into the striatum [9-11,35-39]. Three enzymes are necessary for efficient DA synthesis: tyrosine hydroxylase (TH), aromatic L-amino acid decarboxylase (AADC) and guanosine triphosphate cyclohydrolase I (GCH) (Figure 1). TH is the rate-limiting enzyme that converts L-tyrosine to L-dopa; AADC converts L-dopa to DA; and GCH is the rate-limiting enzyme in the biosynthesis of the essential TH cofactor, tetrahydrobiopterine (BH_4). These three enzymes are synthesised in SNc neurons and are anterogradely transported to the striatum. In advanced PD, the severe loss of dopaminergic nerve terminals is associated with an 80 – 95% depletion of striatal TH and AADC activity [40-42], leading to a profound decrease in DA. Failure to respond to L-dopa therapy may result from a reduction in AADC activity, decreased DA storage capacity in synaptic vesicles, postsynaptic changes in striatal output neurons and/or abnormalities of non-dopaminergic neurotransmitter systems. AADC is present in DA-denervated striatum within non-dopaminergic neurons and glial cells, but endogenous AADC activity in the

striatum is considered insufficient, at least in primates [35,43]. Although L-dopa may function as a neurotransmitter or modify behaviour through DA-independent mechanisms, central inhibition of AADC with 3-hydroxybenzylhydrazine (NSD-1015) has been shown to result in the abolition of the L-dopa motor effect [44], corroborating the classical concept that L-dopa is pharmacologically inert and its effects are mediated by DA and metabolites. Thus, most of the L-dopa produced in the striatum after gene transfer must be converted to DA *in situ*. Along with decreases in the levels of BH_4, TH and DA observed in PD, the activity of GCH in the striatum is also decreased in this disease [45]. As a low level of endogenous BH_4 does not yield sufficient TH activity, GCH is thought to regulate TH activity by regulating BH_4 biosynthesis, thus indirectly controlling DA production in TH-containing DA neurons [45-47]. In dominantly inherited dopa-responsive dystonia, a mutation in the gene encoding GCH results in a decrease in the level of BH_4, a further decrease in TH activity and a decrease in DA production [48]. Although BH_4 can cross the blood–brain barrier, uptake of exogenous BH_4 from the blood is low [49] and the primary source of BH_4 in the brain is via intracellular biosynthesis. Thus, GCH gene transfer into striatal cells may offer a more efficient method of supplying BH_4 than its exogenous administration.

3.2 Dopamine production in animal models

The availability of well-characterised rodent and non-human primate models makes PD a suitable candidate for gene therapy experiments. These models use neurotoxins that selectively elicit DA neuronal death in the SNc and deplete nigrostrital DA. A rat model of PD is generated by injecting 6-hydroxydopamine (6-OHDA) into the striatum or nigrostriatal pathway [50]. Systemic or intracarotid administration of 1-methyl-4-phenyl-1,2,3,6-tetrahydropyridine (MPTP) into monkeys replicates all the cardinal signs of PD, including tremor, rigidity, bradykinesia and postural instability. The primate MPTP model is useful in evaluating motor functions and in assaying transduction efficiency in the larger striatum.

The limited packaging capacity of rAAV vectors (< 5 kb) makes it impossible to use a single vector to express all three enzymes. However, one cell could be simultaneously transduced with multiple rAAV vectors encoding different enzymes. Although the addition of AADC via genetically modified fibroblasts to a system expressing TH and GCH has been reported to result in reduced production of L-dopa, due to feedback inhibition of DA on TH [51,52], direct gene transfer of AADC and TH into the striatum using rAAV vectors has been found to be beneficial in 6-OHDA-lesioned rats [10,36]. Local production of striatal DA was higher in cells expressing GCH, TH and AADC than in cells expressing TH and AADC, and these results have been confirmed in a primate model [38]. rAAV vectors have been shown to efficiently introduce genes encoding DA-synthesising enzymes into the striatum of the MPTP model, resulting in the restoration of motor functions with robust transgene expression and elevated DA synthesis in the treated putamen.

So far, dyskinesia has not been observed in preclinical studies of rAAV vector-mediated gene delivery of DA-synthesising enzymes. Moreover, rAAV vector-mediated delivery of TH and GCH was found to reverse peak-dose dyskinesia in a rat model of PD [53]. Continuous DA production in the striatum may account for the reduced likelihood of dyskinesia. It has been clinically shown that, compared with drugs that have a long duration of effect, short-acting pulsatile DA agonists are more likely to induce dyskinesia in PD patients [5]. Compared with conventional oral therapies, continuous intraduodenal infusion of L-dopa/carbidopa has a greater effect on motor performance improvement, but without increasing dyskinesia [54].

Gene transfer of AADC alone, in combination with oral administration of L-dopa, could be a shortcut to start clinical trials in PD patients [35,39]. Although these patients would still need to take L-dopa to control their PD symptoms, DA production could be regulated by altering the dose of L-dopa. It could be argued that the major reason for failure of L-dopa therapy is that adverse effects overwhelm the therapeutic response (shrinking of the therapeutic window). Many of the late-stage complications of PD result from the very high doses of L-dopa required to induce a therapeutic response. Experimental and clinical experience using inhibitors of catechol-*O*-methyl-transferase (COMT) indicates that a reduction in the dose of L-dopa is important in controlling the dyskinesia associated with prolonged DA half-life [55]. Restoring decarboxylating capacity by gene transfer could potentially allow lower doses of L-dopa and reduce the long-term adverse effects associated with escalating L-dopa therapy [10,35,39,41,56].

4. Protection of the nigrostriatal pathway

An alternative approach to the treatment of PD is to protect the nigrostriatal pathway from progressive degeneration by providing genes encoding growth factors [57], antioxidant molecules or antiapoptotic substances [58]. The slow progressive nature of degeneration in PD makes this approach attractive for arresting or even reversing parkinsonian symptoms. One potential candidate for this strategy is glial cell line-derived neurotrophic factor (GDNF) [57,59], a small glycoprotein that provides strong tropic support for DA neurons [60]. Application of the GDNF protein, however, is limited by its short half-life and its poor ability to cross the blood–brain barrier. An attempt to treat PD patients by direct injection of GDNF protein into the ventricles was unsuccessful [61]. A Phase I safety trial of continuous delivery of GDNF into the postero-dorsal putamen of five PD patients showed alleviation of off-medication motor symptoms and dyskinesia [62], and positron emission tomography (PET) detected increased DA storage, both in the putamen and the substantia nigra, suggesting retrograde transport of GDNF. Delivery of the gene encoding GDNF by viral vectors would be advantageous for PD patients, in that a single injection